Received: 28 April 2024 | Revised: 11 August 2024 | Accepted: 26 August 2024

DOI: 10.1002/dug2.12140

RESEARCH ARTICLE

Corrosion effect of hydrochloric acid on the granite: Insights from electrical conductivity, mineral composition, and tensile behavior

Yanan Gao[1,2] | **Yikang Cheng**[1,2] | **Guanglei Cai**[3] | **Yuan Gao**[4] | **Jianwei Tian**[5] | **Mingzhong Gao**[6]

[1]State Key Laboratory of Intelligent Construction and Healthy Operation and Maintenance of Deep Underground Engineering, China University of Mining and Technology, Xuzhou, China

[2]School of Mechanics and Civil Engineering, China University of Mining and Technology, Xuzhou, China

[3]Department of Civil and Environmental Engineering, The Hong Kong Polytechnic University, Hong Kong, China

[4]School of Chemical Engineering and Technology, China University of Mining and Technology, Xuzhou, China

[5]Danish Offshore Technology Centre, Technical University of Denmark, Lyngby, Denmark

[6]College of Civil and Transportation Engineering, Shenzhen University, Shenzhen, China

Correspondence

Yanan Gao, State Key Laboratory of Intelligent Construction and Healthy Operation and Maintenance of Deep Underground Engineering, China University of Mining and Technology, Xuzhou 221116, China.
Email: yngao@cumt.edu.cn

Funding information

National Science Fund for Distinguished Young Scholars, Grant/Award Number: 52225403; State Key Laboratory of Intelligent Construction and Healthy Operation and Maintenance of Deep Underground Engineering, Grant/Award Number: SDGZK2404; Fundamental Research Funds for the Central Universities, Grant/Award Number: 2023KYJD1006

Abstract

Hydrochloric acid (HCl) extensively exists in deep underground projects, arising from the transportation of industrial raw materials or fracturing fluids of petroleum engineering. It results in corrosion, which can significantly impact the stability of surrounding rock structures. Therefore, in-depth analysis of the degradation of rock corroded by the HCl solution is an essential task for underground engineering. In this study, the granite specimens are initially treated with the HCl solution with various concentrations. Then, the tests and analyses, such as electrical conductivity (EC) measurements, mineral composition assays, and Brazilian splitting tests, are employed to investigate the corrosion mechanism of the HCl solution. Our results and findings are generally as follows: (1) As the immersion time increases, the EC exhibits a relatively high level at pH value of 1, a decreasing trend at pH value of 3, and an increasing trend at pH value of 5 and 7. (2) The HCl solutions with various concentration have different effect on mineral composition, characterized by an increase in proportion of SiO_2 and a reduction in proportion of Na_2O, Al_2O_3, K_2O, MgO, and CaO, as the solution pH value decreases. (3) After immersion in the solutions with pH values of 1, 3, and 5, the tensile strength of the granite decreases by 23.85%, 20.84%, and 20.24%; the average stiffness of the specimen decreases by 29.29%, 23.43%, and 11.97%; the proportion of releasable energy increases by 6%, 4%, and −2%; the releasable energy decreases by 54.96%, 26.09%, and 14.52%; and the dissipated energy decreases by approximately 68.85%, 41.39%, and 5.41%, respectively. (4) The evolution of physical and mechanical properties of the immersed granite specimen can be analyzed from a chemical aspect. The corrosive action of HCl cleaves Si–O and Al–O chemical bonds within the granite, particularly altering the tetrahedral structures of its silicate components. This process involves breaking existing chemical bonds and the formation of new ones, ultimately destroying the silicate molecular structures. As the concentration of HCl increases, the rate of these reactions accelerates, progressively weakening the chemical bonds and consequently deteriorating the mechanical characteristics of the granite. These findings can deepen our knowledge about the corrosion effect of HCI solutions on natural surrounding rocks and serve as references for further research on rock corrosion mechanisms in underground engineering.

KEYWORDS

corrosion effect, electrical conductivity, HCl solution, mineral composition, tensile behavior

Highlights

- The study investigates how the electrical conductivity of the solution for immersing the granite specimen changes under various HCl conditions.

- The mineral composition of the granite specimen across the different HCl treatments is analyzed and quantified.
- The tensile behavior and the energy evolution of the granite specimens during the Brazilian splitting test are examined, with a particular focus on the effect of different HCl conditions.
- The mechanism driving the changes in the physical properties is interpreted and discussed from a chemical perspective.

1 | INTRODUCTION

The impacts of complex geological environments, such as high temperature, high pressure, and acidic/alkaline conditions, become increasingly significant as underground engineering advances to greater depths. HCl is widely used as a common industrial raw material and serves as the primary component of fracturing fluids in petroleum engineering. The effect of acid corrosion on rock induced by industrial wastewater can be considered as a chemical process (Figure 1). In addition, such corrosion can lead to the degradation of the mechanical properties of rock and influence the stability of underground engineering. Meanwhile, underground engineering projects, such as basement, tunnel, and mining often lead to the change of stress state of surrounding rocks (Dai et al., 2024). It is well known that the tensile strength of rock is much lower than the compressive strength. Therefore, it is necessary to investigate the tensile strength of rock corroded by HCl solution with various concentrations.

Numerous scholars have widely studied the variations in the physical and mechanical properties of rocks under complex acid conditions. For example, the mechanical properties, including elastic modulus, shear modulus, and indirect tensile strength, generally decreased due to acid corrosion (Alameedy et al., 2023; Nouailletas et al., 2017; Tariq et al., 2021). Marangu (2021) and Taghipour et al. (2016) revealed that the compressive strength of limestone decreases as the concentration of the acid solution increases. Grandclerc et al. (2018) and Van den Eynde et al. (2013) investigated the corrosive effects of acidic solutions on silicate and carbonate minerals and pointed out a significant influence of the dissolution processes on the porosity of carbonate and evaporitic rocks.

Recent studies present the relationship between the pH value of the acidic solution, reaction time, and the degree of corrosion. Wang et al. (2023) conducted the impact of acid concentration and immersion time on the mechanical properties of rocks. When the specimen was treated with an acid solution, the tensile strength decreased by up to 84%, Young's modulus decreased by up to 63.6%, and Poisson's ratio decreased by up to 40.7%. Based on triaxial compression, Chen, Chen et al. (2023) studied the mechanical properties of sandstone corroded by solution with different pH values. After pH = 1 and a high temperature of 900°C, the mass, wave velocity, and porosity of the sandstone decreased by 1.12%, 23.79%, and 2.58%, respectively.

The correlation between the mechanical properties of rocks and the concentration of acid solution is also investigated extensively. It is well known that the higher the concentration of acid, the greater the degree of rock corrosion. For example, Fan et al. (2023) and Li, Chen, et al. (2019) revealed the reaction mechanism between acids and rocks under various acid concentration conditions. When the acid concentration increased from 12% to 24%, the rate of the acid rock reaction rose correspondingly by approximately 50%. Tao et al. (2022) investigated the

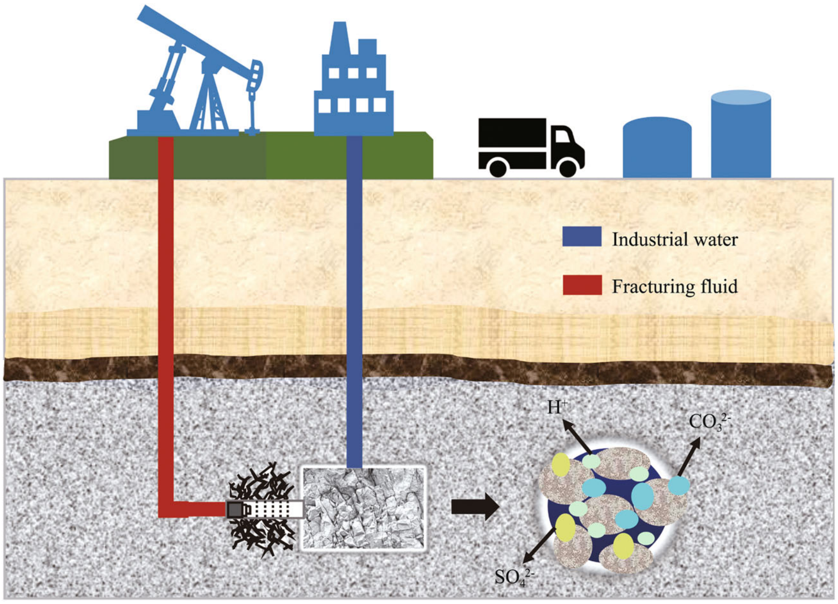

FIGURE 1 Illustration of acid corrosion to rock induced by industrial wastewater.

marble corroded with acid solutions of varying pH values and found that the compression strength and elastic modulus of the rock specimen decreased as the acidity of the acid corrosion increased.

Furthermore, people investigate the correlation between the mechanical properties of rocks and the reaction time of acidic solution. The longer the contact time with the acidic solution, the greater the degree of rock corrosion. Based on uniaxial compression test results, acoustic emission monitoring, and X-ray diffraction experiments, Yu et al. (2023) investigated the mechanical properties of granite under varying durations of corrosion. As the duration of corrosion increased, there was a 25.6% decrease in the uniaxial compressive strength and a 38.3% decrease in the elastic modulus. Li, Yu, et al. (2017) and Zhang et al. (2020) immersed limestone in an acidic solution with a pH value of 3 for varying durations to investigate its dynamic mechanical properties. As the corrosion time increased, the porosity of limestone increased from 0.32% in its natural state to 5.32% after 150 days, and the degree of deterioration in tensile strength was found to be 32.52%. Chen, Wang et al. (2023) and revealed the relationship between the immersion time of acid solution and the compressive strength of coal-rock assemblages. The longer the immersion time, the greater the damage and deterioration of the specimen, resulting in lower strength and stability.

Besides, there are also findings about the electrical conductivity (EC) and mechanical properties of rock. Han et al. (2015) investigated the effect of parameters, that is, porosity, grain aspect ratio, and water saturation on the EC of the sandstone. The study reveals that porosity is the dominant parameter in affecting the electrical properties. Glover et al. (2000) investigated the complex EC measurements of sandstone and found that the frequency dependence of the EC was not significantly affected in these sedimentary rock specimens with moderate porosity and high permeability.

The aforementioned studies have revealed the reaction mechanism and weakening effect on rock caused by acid. However, there is not much attention given to the corrosive effect of acid on the mechanical properties of rock and chemical bonds. It is well known that the variation of the chemical bond may appear when the rock is corroded by acid. Meanwhile, such change could induce variation in physical properties, such as electrical conductivity, mineral composition, and mechanical behavior. Therefore, a more comprehensive understanding of the mechanism of physical properties of rock under acidic conditions is demanded. In this study, granite is selected as the research subject due to its widespread distribution in underground engineering and its high hardness. Then, a series of tests and analyses are conducted on the specimens treated with HCl solution at different pH values, including electrical conductivity, mineral composition analysis, and the Brazilian splitting test. Finally, the mechanism behind the evolution of the physical properties is examined from a chemical perspective.

2 | EXPERIMENTAL DESIGNS

2.1 | Specimen preparation

The rock specimens used in this study are homogeneous granites from Linyi, Shandong Province, China. The granite blocks are manufactured into cylindrical specimens with a diameter of 50 mm, and a height of 25 mm, in accordance with the ISRM standard for rock specimen preparation. The upper and lower end faces of the specimens are meticulously polished to ensure precise parallelism and perpendicularity, with an error margin of less than 0.2 mm. These specimens are then divided into four groups, that is, A-*i*, B-*i*, C-*i*, and D-*i* ($i = 1–2$). The mass and geometry information is listed in Table 1. It is worth noting that the concentration of the solution of group D is 0, that is, pH = 7, and group D is set as the reference group to analyze the damage degree of the specimens corroded by acid solution with different concentrations.

2.2 | Experimental procedure

The ion concentration adjustment method is employed to prepare a 10 mol/L HCl solution. Then the HCl solution is used to prepare four acidic solutions with

TABLE 1 Experimental design of the corrosion test.

Sample ID	Size (mm)		Mass (g)	Chemical solution (mol/L)		Immersion time (days)
	Diameter	Height		pH value	HCl concentration	
A-1	49.90	24.88	124.116	1	0.100	23
A-2	49.84	24.72	123.787			
B-1	49.92	25.60	127.989	3	0.010	
B-2	49.82	24.42	123.395			
C-1	49.82	25.70	128.088	5	0.001	
C-2	49.82	25.02	125.190			
D-1	49.96	25.10	124.846	7	0.000	
D-2	49.98	25.30	126.433			

pH values of 1, 3, 5, and 7, which is typically used in experiments to reveal the corrosion effect of rock (Huo et al., 2020). Afterward, each specimen is immersed in an acidic solution for a period of 23 days. The electrical conductivity of the HCl solution is measured every 24 h during this experiment process. Next, the mechanical properties of the specimens are evaluated through Brazilian splitting tests using the MTS816 servo system. Finally, the fragment of the specimen is finely ground and processed into preforming for the analysis of mineral composition.

The specific experiment procedure is as follows:

1. Dilute concentrated HCl with purified water to prepare HCl solutions of pH values 1, 3, and 5, and prepare the solution with a pH value of 7 using a chemical treatment.
2. The specimens in each group are immersed in the corresponding solution.
3. Measure the electrical conductivity of the HCl solution by using a waterproof EC/total dissolved solids (TDS) tester with a frequency of 24 h.
4. After being immersed in the HCl solution for 23 days, the specimens are in preparation for the Brazilian splitting test.
5. Grind the fragments of specimens after mechanical tests into fine powder, and prepare the preforming using the powder metal press.
6. Employ a spectrometer to conduct mineral composition analysis.

The procedure mentioned above is illustrated in Figure 2.

3 | RESULTS AND DISCUSSIONS

3.1 | EC variation of HCl solutions due to corrosion

The measurement of EC is a prevalent technique that can effectively indicate the concentration of salts in water and reflect the corrosive effect of the HCl solutions on rocks. The variations in EC of the HCl solutions with different pH values are depicted in Figure 3. The evolution of the EC of group B, group C, and group D can be divided into three stages: Stage I: the EC increases or decreases rapidly; Stage II: the EC changes slowly; Stage III: no significant variations in EC can be observed.

The initial EC of the solutions at pH values of 1, 3, 5, and 7 are 9.99, 468.00, 75.50, and 77.30 μs/cm, respectively. For group A ($pH = 1$), it is worth noting that the EC remains unchanged, it may be due to the measuring range of the EC/TDS tester. For group B ($pH = 3$), the EC exhibits a linear decrease. After 9 days of immersion, there is a significant drop of approximately 5.7%, ultimately reaching a value of 383 μs/cm. In contrast to this trend, at a pH value of 5 (group C), the EC exhibits an almost linear upward trajectory. However, it experiences a sudden decline of approximately 2.2% after 20 days of immersion. Subsequently, it gradually increases once again and then stabilizes at around 138 μs/cm. At a pH value of 7 (group D), there is a nearly linear increase in EC. Similar to group C, there is a sudden decrease of 4.2% after 20 days of immersion, followed by a gradual recovery and stabilization around 144 μs/cm.

The EC of the HCl solution is attributed to the presence of free ions. The higher the concentration of

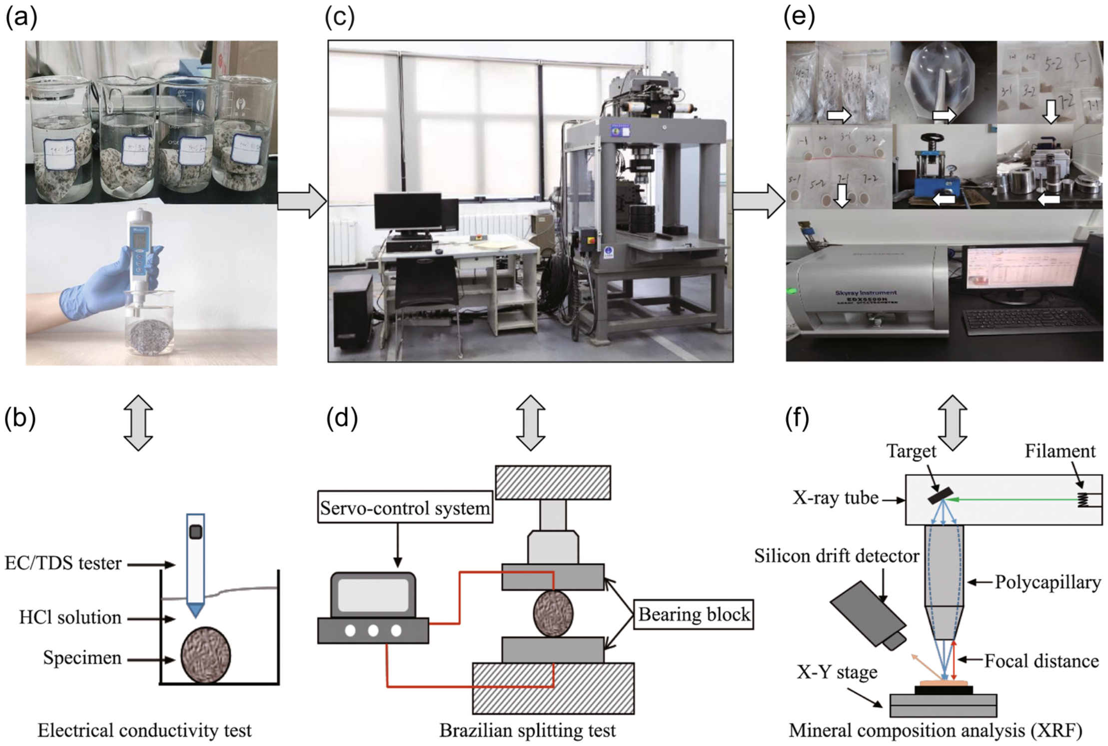

FIGURE 2 Illustration of experimental procedure. (a, b) Facility and schematic diagram of EC test. (c, d) Facility and schematic diagram of Brazilian splitting test. (e, f) Facility and schematic diagram of mineral composition analysis (f is modified after Aida et al. [2017]). XRF, X-ray fluorescence spectrometer.

dissolved salt in the HCl solution, the greater the number of ions present, resulting in an increased EC of the HCl solution. The EC of the granite gradually increases when it is immersed in the HCl solution with a lower concentration. However, the EC gradually decreases in solution with higher concentration. It can be observed that there are no significant variations in the EC of the HCl solution in each group when the specimens are immersed in the solution from 17 to 23 days. Therefore, it can be considered that the majority of H^+ and Cl^- ions of the HCl solution in each group have sufficiently reacted with the granite. Both the granite and the HCl solution in each group have reached a relatively stable state.

3.2 | Mineral composition variation of granite material due to corrosion

X-ray fluorescence (XRF) spectrometer is used to measure the mineral composition of the granite in each group. ZSX Primus IV instrument is used in the experiment. It is composed of four optical filters, and the thickness of the beryllium window is less than 50 µm. As mentioned in Section 2.2, before measuring the mineral composition of the granite with XRF, a preforming of the specimen should be prepared. Firstly, the fragments of the fracture specimens are collected and ground into a powder with a particle size of less than 0.3 mm. Subsequently, the boric acid mold and powder metal press are used to prepare the preforming. Finally, the XRF spectrometer is used to determine the mineral composition of the granite under different corrosion conditions.

The change in the mineral composition of the granite induced by the HCl solution is shown schematically in Figure 4. And SiO_2, Al_2O_3, K_2O, Na_2O, CaO, and MgO all react with HCl solution. The composition of the granite mainly consists of SiO_2, Al_2O_3, K_2O, Na_2O, CaO, and MgO (Figure 5). Immersion in relatively high-concentration HCl solutions may result in a significant increase in the proportion of SiO_2. However, the amount of other mineral compositions decreases. In detail, compared to being immersed in the solution with a pH value of 7, the SiO_2 content increased by 0.72% and 2.89% after immersion in the HCl solutions with pH values of 1 and 3. The contents of Al_2O_3, MgO, CaO, Na_2O, and K_2O decrease by 0.24%, 0.05%, 0.08%, 0.05%, and 0.49%, respectively. However, the effect of a relatively low concentration of HCl solution on mineral composition is found to be negligible. Additionally, the mass of the specimen increases after being immersed in an HCl solution (Figure 6). Furthermore, it should be noted that the silica proportion also increases if the specimen is immersed in such a solution.

3.3 | Tensile behavior change of granite specimens due to corrosion

In the Brazilian splitting test, a thin disc specimen is assumed to be loaded with a uniform pressure that is radially applied over a short strip of the circumference at each end of a diameter (Erarslan & Williams, 2012a). An

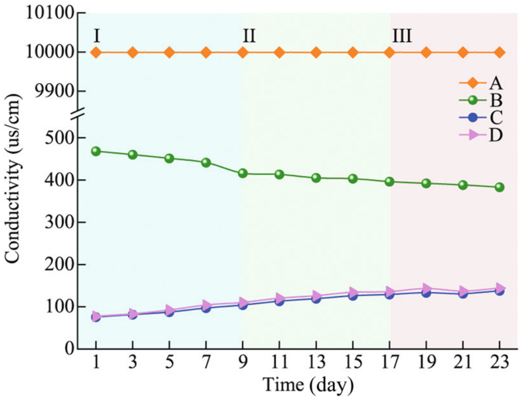

FIGURE 3 Electrical conductivity variation of the solutions after immersion of the specimens.

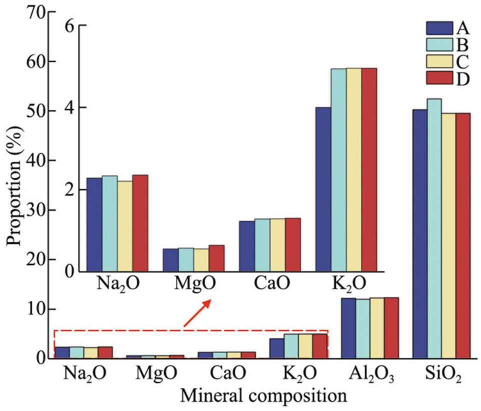

FIGURE 5 The proportion of the mineral composition in different groups.

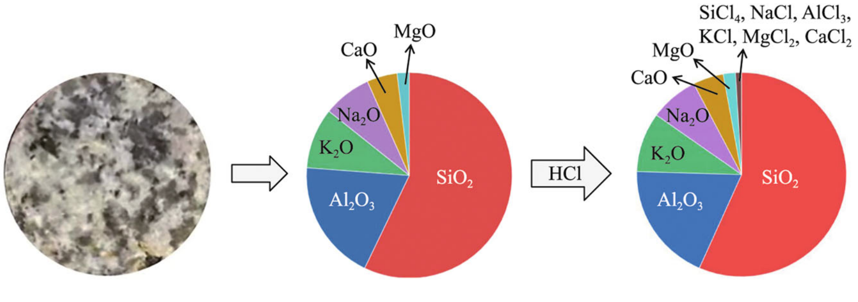

FIGURE 4 The change of the mineral composition of the specimen induced by the HCl solutions.

important and fundamental assumption for determining the tensile strength of rocks and rock-like materials through the Brazilian splitting test is that the material is considered homogeneous, isotropic, and linearly elastic before brittle failure (Fuenkajorn & Klanphumeesri, 2011).

The Brazilian splitting test is widely employed to measure the tensile strength of rock for its simplicity of operational and accurate assessment (Erarslan & Williams, 2012b). The corrosion effect of HCl solutions on the tensile strength of the granite can be determined via the Brazilian splitting tests of the immersed specimens. Thus, those results can provide a scientific reference for the assessment of rock stability in underground engineering.

The Brazilian splitting test relies on applying radial compressive loads to induce maximum tensile stress in the specimen. The equation for calculating tensile stress is known as follows:

$$\sigma = \frac{2P}{\pi DT}, \tag{1}$$

where σ represents the tensile stress of the granite, MPa; P represents the force applied by the loading system, N; D represents the diameter of the granite, mm; T represents the thickness of the granite, mm.

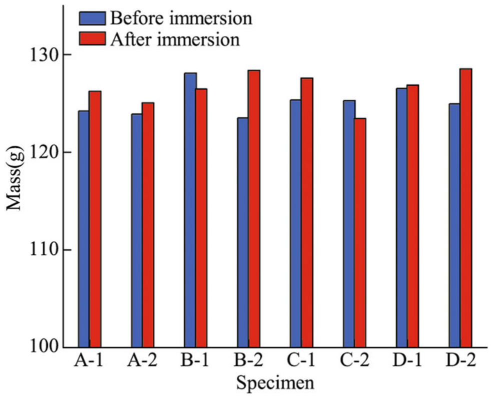

FIGURE 6 Mass change of the specimens after immersion into HCl solutions.

3.3.1 | Load−displacement relationship

In this study, the MTS816 electro-hydraulic servo mechanical testing machine is used to measure the tensile strength of the specimens. The loading rate is set as 0.002 mm/s.

During the loading process, the specimens undergo three distinct stages: linear elastic deformation, plastic yielding, and failure (Yang et al., 2023). In the linear elastic stage, stress rapidly increases as strain accumulates. Subsequently, during the plastic-yielding stage, the slope gradually decreases while approaching the material threshold, leading to microcrack formation within the granite. Finally, in the failure stage, stress steadily decreases with increasing strain as the main crack propagates through the entire specimen, resulting in ultimate failure.

Additionally, the increase in the concentration of the HCl solution results in a decrease in both the duration of linear elastic deformation and peak strength, thereby reducing the load-carrying capacity. The tensile strength of the specimens is summarized in Table 2. The average tensile strength of the specimens at pH values of 1, 3, 5, and 7 is recorded and calculated as 3.80, 3.95, 3.98, and 4.99 MPa, respectively. It is evident that the tensile strength of the granite gradually decreases as the concentration of the HCl solution increases. As shown in Figure 7, the tensile strength of the granite decreases by 23.85% at the pH value of 1, by 20.84% at the pH value of 3, and by 20.24% at the pH value of 5. It can be concluded that the mechanical properties of granite may exhibit a significant degradation under the corrosion of the HCl solutions. It is imperative to consider the impact of an acidic environment when analyzing the stability of surrounding rock in underground engineering.

3.3.2 | Average stiffness

The Young's modulus cannot be reliably determined in the Brazilian splitting test due to the uneven distribution of stress in the specimen. However, the applied load and the displacement of the upper bearing block of the loading machine can be used to evaluate the stiffness of the specimen. The average gradient of the load−displacement

TABLE 2 Tensile strength results.

Specimen ID	pH value	Size (mm)		Tensile strength (MPa)		Damage ratio (%)
		ΔD	ΔH	Peak strength	Average	
A-1	1	0.00	−0.22	3.10	3.80	76.15
A-2		0.06	−0.24	4.50		
B-1	3	−0.04	0.26	3.95	3.95	79.16
B-2		0.08	−0.88	/		
C-1	5	0.10	1.12	4.77	3.98	79.76
C-2		0.00	−0.26	3.18		
D-1	7	−0.06	−0.40	5.40	4.99	100.00
D-2		−0.08	0.12	4.57		

Note: Slash (/) represents invalid data. ΔD and ΔH represent the change in diameter and height of the specimen.

curve represents the average stiffness of the specimen (Wong & Jong, 2014). The average stiffness of the specimen for each concentration of HCl solution is shown in Table 3.

The load–displacement curves of the specimens corroded by HCl solutions are shown in Figure 8. The average stiffness of the specimens of group D (pH = 7) is 32.09 kN/mm, but that of specimens immersed in HCl solutions with pH values of 1, 3, and 5 is 22.69, 24.57, and 28.25 kN/mm, respectively. It is evident that the lower the pH value, the lower the average stiffness. The average stiffness of the granite decreases by 29.29% at the pH value of 1, by 23.43% at the pH value of 3, and by 11.97% at the pH value of 5. The stiffness of the specimen is related to its Young's modulus since it represents the property of deformation resistance. Therefore, it can be inferred that the corrosion effect caused by acid may decrease the Young's modulus of the granite.

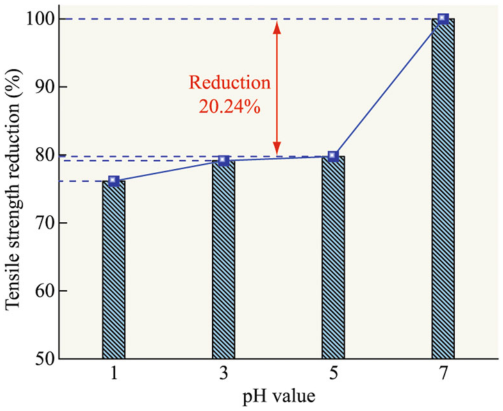

FIGURE 7 Tensile strength reduction of the specimens corroded by the HCl solutions.

TABLE 3 Average gradient of the load–displacement curves of the specimens corroded by the solutions.

pH value	1	3	5	7
Average gradient (kN/mm)	22.69	24.57	28.25	32.09
Standard deviation	1.94	2.36	2.99	3.25

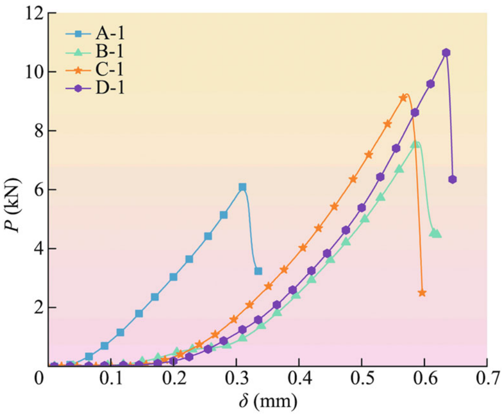

FIGURE 8 Typical load–displacement curves of the specimens corroded by the HCl solutions.

3.3.3 | Releasable energy and dissipated energy

It is well known that there is an energy transfer and transformation during the loading and failure process. Quantitative analysis of the energy behavior can reveal the deformation and failure mechanism of the specimens subjected to the HCl corrosion.

According to the point of conservation of energy, the relationship between the work of the external force and energy can be described as follows:

$$W = U + V, \tag{2}$$

$$W = \int_0^{\delta_1} P \mathrm{d}\delta, \tag{3}$$

where W represents the work of the external force, U represents the releasable energy of the specimen, V represents the dissipated energy of the specimen, P represents the force applied by the loading system, and δ_1 represents the displacement of the upper bearing block.

The relationship between releasable energy and dissipated energy, as well as total work, is illustrated in Figure 9. The dissipated energy is irreversible as it is associated with rock damage, such as crack initiation or propagation. However, the releasable energy may disappear when the loading pressure is relieved. According to previous research, it can be observed that the average slope of the unloading curve typically aligns with the average slope of the loading curve (Feng et al., 2005). Therefore, the releasable energy can be calculated using the following equation:

$$U = \frac{1}{2} P\delta_2, \tag{4}$$

where δ_2 represents the overall displacement minus the displacement after the loading pressure is relieved.

Then, the dissipated energy can be calculated using the below equation:

$$V = \int_0^{\delta_1} P \mathrm{d}\delta - \frac{1}{2} P\delta_1. \tag{5}$$

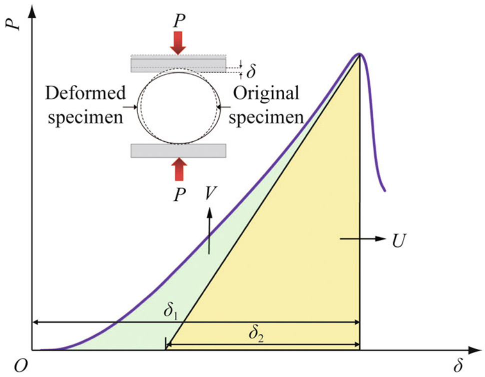

FIGURE 9 Illustration of releasable energy and dissipated energy (U stands for releasable energy and V stands for dissipated energy).

The change of releasable energy and dissipated energy of the granite subjected to HCl solutions with different pH values is shown in Figure 10. The releasable energy of the specimen immersed in the solution with a pH value of 7 is 1.25 J, but that of specimens immersed in the solutions with pH values of 1, 3, and 5 is 0.56, 0.92, and 1.07 J, respectively. The dissipated energy of the granite treated by the solutions with pH values of 1, 3, 5, and 7 is 0.15, 0.28, 0.45, and 0.47 J, respectively. The decrease in pH value, that is, the increase in the concentration of the solution, may result in a decrease in both releasable energy and dissipated energy. Figure 10 also shows the proportion of changes in releasable energy and dissipated energy. The proportion of releasable energy of the granite increases by 6% at the pH value of 1, by 4% at the pH value of 3, and by −2% at the pH value of 5. Generally, the lower the pH value, the greater the increase in releasable energy. Similar conclusions can be obtained through the results of the dissipated energy. Additionally, there is a nearly linear relationship between releasable energy and the pH value of the solution.

Figure 11 shows the reduction of releasable energy and dissipated energy. The reduction ratio of the releasable energy of the granite decreases by 54.96% at the pH value of 1, by 26.09% at the pH value of 3, and by 14.52% at the pH value of 5. It is evident that the lower the pH value, the greater the reduction in releasable energy. There is a nearly linear relationship between releasable energy and the pH value of the HCl solution. The dissipated energy of the specimen decreases by 68.85% at the pH value of 1, by 41.39% at the pH value of 3, and by 5.41% at the pH value of 5. Thus, the dissipated energy of the specimen is not affected very much by the HCl solution with a pH value of 5.

The dissipated energy is a fundamental characteristic of rock deformation and failure. It reflects the progressive development of micro-defects within the rock matrix. The strength gradually decreases until it is destroyed (Cao et al., 2020). Consequently, energy dissipation directly correlates with damage and strength loss. The magnitude of dissipated energy can be used as an indicator for the degree of failure of rock (Xie et al., 2005). The corrosion of the solution on the granite results in a significant reduction of dissipated energy, leading to great damage. Hence, besides the degradation of mechanical properties, the view of energy can be taken as another approach to interpreting the corrosion effect of the HCl solutions.

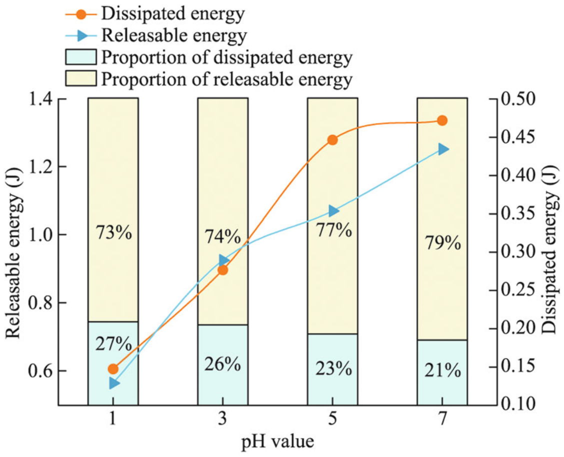

FIGURE 10 Variations in releasable energy and dissipated energy of the specimens corroded by the HCl solutions.

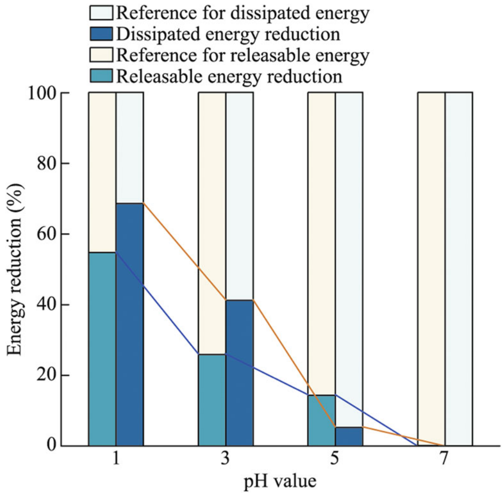

FIGURE 11 The reduction of releasable energy and dissipated energy of the specimens corroded by the HCl solutions.

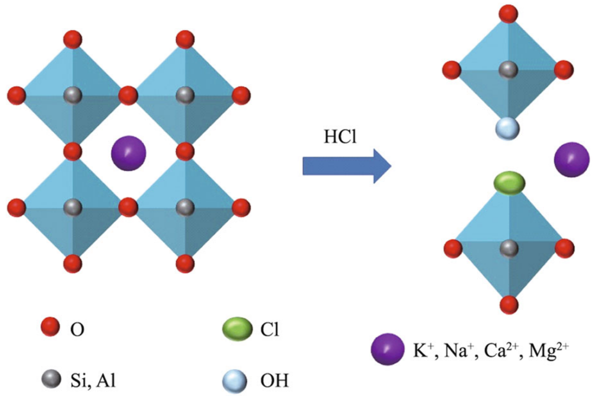

FIGURE 12 Schematic diagram of influence of HCl on microstructure.

4 | DISCUSSION

The microstructure of granite is primarily composed of covalent bonds, including Si–O, Al–O, Si–OH, and Al–OH, as well as the ionic bonds involving K^+, Na^+, Ca^{2+}, and Mg^{2+}. The main structural units in granite are (Si–O) tetrahedrons and (Al–O) octahedrons. When granite interacts with the HCl solution, changes in its microstructure occur, as illustrated in Figure 12. The ions within these structural units are exchangeable, and hydroxylation occurs at the mineral lattice surfaces in the presence of the HCl (Li et al., 2016).

The mechanism of chemical bonding reactions of silicate minerals is detailed in Figure 13. In these reactions, the M atom represents either a Si or Al. Both the covalent bonds (e.g., M–O and M–OH) and ionic bonds in granite minerals react with HCl. Generally, covalent bonds are stronger than ionic bonds. The quartz

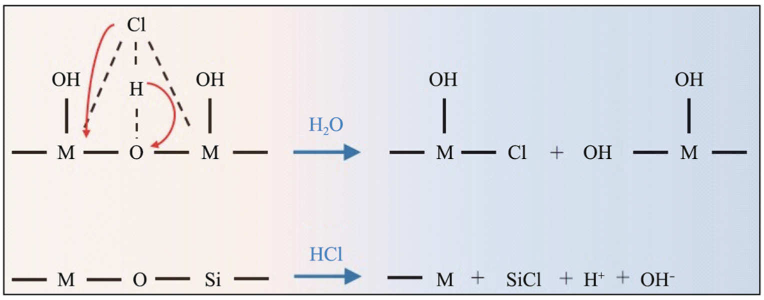

FIGURE 13 The change of chemical bonds.

in the granite, which contains covalent bonds M–O, has the slowest dissolution rate, indicating that the cleavage of the covalent bonds M–O is significant during the reaction between HCl and siliceous mineral (Blumberg & Stavrinou, 1960; Fogler et al., 1975).

Based on the test results in this study, it can be generally accepted that the corrosion effect of the HCl solution on the granite induces significant changes in its mass, mineral composition, microstructure, and mostly mechanical properties. After immersion in HCl, there is an observable increase in the mass of granite, along with a rise in SiO_2 content, while the concentrations of Na_2O, Al_2O_3, K_2O, MgO, and CaO decrease. This dissolution of silicate minerals contributes to an elevated salt concentration in the solution, thereby increasing its EC. As mentioned above in the discussion, the chemical bonds, specifically Si–O and Al–O, undergo cleavage due to the corrosive action of HCl, leading to a reconfiguration of the molecular structure of the silicates. This process involves breaking original chemical bonds and forming new ones, ultimately destroying the molecular structure of the silicates. By comparing results from four groups using solutions of various pH values in our tests, an increase in acid concentration can possibly accelerate these chemical reactions, further weakening the chemical bonds and exacerbating the degradation of the mechanical properties of the granite.

5 | CONCLUSIONS

In this study, the specimens are initially treated with HCl solutions of different pH values. Subsequently, a series of tests and analyses, such as EC, mineral composition, and tensile strength of the granite specimens are conducted to investigate the corrosion mechanism of the HCl solution. Finally, the microscopic mechanism of the corrosion effect is discussed in the view of chemical bonds.

1. The EC can reflect the change in the salt concentration of the HCl solutions. The concentration of the ionic species is a key factor in the conductivity of the solution. After immersion in the solutions with pH values of 1, 3, 5, and 7, at pH value of 1, the EC value remains at a high level, and it may be due to the measuring range of the EC/TDS tester. At a pH value of 3, the EC gradually decreases. At pH values of 5 and 7, the EC gradually increases. Finally, the EC gradually showed no significant variations.
2. After being immersed in the solutions, there is a significant increase in silica composition, while the proportion of other mineral compositions decreases. After being corroded by a solution of high concentration of HCl, the SiO_2 content increases by 0.72%, while the Al_2O_3, MgO, CaO, Na_2O, and K_2O contents decrease by 0.24%, 0.05%, 0.08%, 0.05%, and 0.49%, respectively. However, the impact on substance content caused by a solution of low concentration of HCl is relatively insignificant.
3. The tensile strength, stiffness, and energy of the specimen decrease with an increase in the concentration of the HCl solution. After being immersed in the solutions with pH values of 1, 3, and 5, the tensile strength of the specimen decreases by 23.85%, 20.84%, and 20.24%, respectively. The stiffness of the specimen decreases by 29.29%, 23.43%, and 11.97% respectively. Additionally, the proportion of releasable energy increases by 6%, 4%, and −2%, respectively; the releasable energy decreases by 54.96%, 26.09%, and 14.52%, and the dissipated energy decreases by approximately 68.85%, 41.39%, and 5.41%, respectively. It is evident that immersion in the HCl solution significantly affects the mechanical properties of the granite.
4. The corrosive action of HCl cleaves the Si–O and Al–O chemical bonds within the granite, particularly affecting the silicate tetrahedral structure. This process breaks the original chemical bonds and facilitates the establishment of new ones, ultimately destroying the silicate tetrahedral arrangement. With increasing acid concentration, the rate of these chemical reactions accelerates, further weakening the chemical bonds and deteriorating the mechanical characteristics of the granite.

AUTHOR CONTRIBUTIONS

Yanan Gao: Conceptualization; methodology; software; supervision; writing—original draft; review and editing. **Yikang Cheng**: Conceptualization; methodology; resources; software; writing—original draft. **Guanglei Cai**: Methodology; supervision; writing—review and editing. **Yuan Gao**: Methodology; supervision; writing—review and editing. **Jianwei Tian**: Software; writing—review and editing. **Mingzhong Gao**: Supervision; writing—review and editing.

ACKNOWLEDGMENTS

This project is supported by the National Science Fund for Distinguished Young Scholars (52225403), Fundamental Research Funds for the Central Universities (2023KYJD1006), and State Key Laboratory of Intelligent Construction and Healthy Operation and Maintenance of Deep Underground Engineering (SDGZK2404).

CONFLICT OF INTEREST STATEMENT

The authors declare no conflict of interest.

DATA AVAILABILITY STATEMENT

The data that support the findings of this study are available from the corresponding author upon reasonable request.

REFERENCES

Aida S, Matsuno T, Hasegawa T, Tsuji K. Application of principal component analysis for improvement of X-ray fluorescence images obtained by polycapillary-based micro-XRF technique. *Nucl Instrum Methods Phys Res Sec B Beam Interact Mater Atoms*. 2017;402:267-273.

Alameedy U, Fatah A, Abbas AK, Al-Yaseri A. Matrix acidizing in carbonate rocks and the impact on geomechanical properties: a review. *Fuel*. 2023;349:128586.

Blumberg AA, Stavrinou SC. Tabulated functions for heterogeneous reaction rates: the attack of vitreous silica by hydrofluoric acid. *J Phys Chem*. 1960;64(10):1438-1442.

Cao K, Ma L, Wu Y, Khan NM, Yang J. Using the characteristics of infrared radiation during the process of strain energy evolution in saturated rock as a precursor for violent failure. *Infrared Phys Technol*. 2020;109:103406.

Chen JX, Wang SJ, Zhang H, Hu SS, Liu P, Zhang JW. Corrosion characteristics and dynamic properties of the coal-rock combination under hydrochemical condition. *J China Univ Min Technol*. 2023;52(5):952-962.

Chen Q, Chen Y, Xiao P, Du X, Pan Y, Azzam R. Mechanical properties and damage constitutive model of sandstone after acid corrosion and high temperature treatments. *Int J Min Sci Technol*. 2023;33(6):747-760.

Dai LP, Pan YS, Xiao YH, et al. Parameter design method for destressing boreholes to mitigate roadway coal bursts: theory and verification. *Rock Mech Rock Eng*. 2024;57:9539-9556. doi:10.1007/s00603-024-04042-x

Erarslan N, Williams DJ. Investigating the effect of cyclic loading on the indirect tensile strength of rocks. *Rock Mech Rock Eng*. 2012a;45(3):327-340.

Erarslan N, Williams DJ. Experimental, numerical and analytical studies on tensile strength of rocks. *Int J Rock Mech Min Sci*. 2012b;49:21-30.

Van den Eynde VC, Mateos FJ, Paradelo R. Degradability of building stone: influence of the porous network on the rate of dissolution of carbonate and evaporitic rocks. *J Cult Herit*. 2013;14(2):89-96.

Fan Y, Peng H, Chen G, et al. Experimental study of the influences of different factors on the acid-rock reaction rate of carbonate rocks. *J Energy Storage*. 2023;63:107064.

Feng P, Ye LP, Huang YL. Deformability and new performance indices of flexural members. *Eng Mech*. 2005;6:28-36.

Fogler HS, Lund K, McCune CC. Acidization III: the kinetics of the dissolution of sodium and potassium feldspar in HF/HCl acid mixtures. *Chem Eng Sci*. 1975;30(11):1325-1332.

Fuenkajorn K, Klanphumeesri S. Laboratory determination of direct tensile strength and deformability of intact rocks. *Geotech Test J*. 2011;34(1):97-102.

Glover PWJ, Gómez JB, Meredith PG. Fracturing in saturated rocks undergoing triaxial deformation using complex electrical conductivity measurements: experimental study. *Earth Planet Sci Lett*. 2000;183(1/2):201-213.

Grandclerc A, Dangla P, Gueguen-Minerbe M, Chaussadent T. Modelling of the sulfuric acid attack on different types of cementitious materials. *Cem Concr Res*. 2018;105:126-133.

Han T, Clennell MB, Pervukhina M. Modelling the low-frequency electrical properties of pyrite-bearing reservoir sandstones. *Marine Pet Geol*. 2015;68:341-351.

Huo RK, Qiu T, Liang YL, Li SG, Qian MT. The physicomechanical deterioration characteristics and mesoscopic damage analysis of sandstone under acidic environment. *Adv Civil Eng*. 2020;2020:7467608.

Li GL, Yu YL, Jing HW, Su HJ, Zhang T, Li M. Experimental study of dynamic compressive mechanical properties of limestone after acid corrosion. *Rock Soil Mech*. 2017;38(11): 3247-3254.

Li N, Zeng F, Li J, Zhang Q, Feng Y, Liu P. Kinetic mechanics of the reactions between HCl/HF acid mixtures and sandstone minerals. *J Nat Gas Sci Eng*. 2016;34:792-802.

Li Q, Chen W, Lu Y, Xiao Q. Etched surface morphology analysis experiments under different reaction rates. *J Pet Sci Eng*. 2019;172:517-526.

Marangu JM. Effects of sulfuric acid attack on hydrated calcined clay-limestone cement mortars. *J Sustainable Cement-Based Mater*. 2021;10(5):257-271.

Nouailletas O, Perlot C, Rivard P, Ballivy G, La Borderie C. Impact of acid attack on the shear behaviour of a carbonate rock joint. *Rock Mech Rock Eng*. 2017;50(6):1439-1451.

Taghipour M, Nikudel MR, Farhadian MB. Engineering properties and durability of limestones used in persepolis complex, Iran, against acid solutions. *Bull Eng Geol Environ*. 2016;75(3):967-978.

Tao M, Wang J, Zhao HT, Peng K, Shi Y, Cao WZ. The influence of acid corrosion on dynamic properties and microscopic mechanism of marble. *Geomech Geophys Geo-Energy Geo-Resour*. 2022;8:36.

Tariq Z, Hassan A, Al-Abdrabalnabi R, Aljawad MS, Mahmoud M. Comparative study of fracture conductivity in various carbonate rocks treated with GLDA chelating agent and HCl acid. *Energy Fuels*. 2021;35(23):19641-19654.

Wang L, Jia W, Xu Y, Mou J, Liao Z, Zhang S. Case study on the effect of acidizing on the rock properties of the mahu conglomerate reservoir. *Processes*. 2023;11(2):626.

Wong LNY, Jong MC. Water saturation effects on the Brazilian tensile strength of gypsum and assessment of cracking processes using high-speed video. *Rock Mech Rock Eng*. 2014;47(4):1103-1115.

Xie HP, Ju Y, Li LY. Criteria for strength and structural failure of rocks based on energy dissipation and energy release principles. *Chin J Rock Mech Eng*. 2005;17:3003-3010.

Yang RZ, Xu Y, Liu JX, Ding JF, Cheng L. Static compression behavior and stress-strain relationship of rigid-flexible combinations under cyclic loading-unloading. *Chin J Rock Mech Eng*. 2023;42(Sup2):4216-4236.

Yu Y, Wang ZH, Tang CX. Energy evolution and fractal characteristics of acid corroded granite under uniaxial compression. *Rock Soil Mech*. 2023;44(7):1971-1982.

Zhang ZQ, Wei LY, Li GL, Su HJ, Jing HW. Experimental research on dynamic tensile mechanics of limestone after chemical corrosion. *Chin J Geotech Eng*. 2020;42(6):1151-1158.

AUTHOR BIOGRAPHY

Dr. Yanan Gao is a professor of mechanics and civil engineering, and the assistant director of nonlinear mechanics for rock engineering at the State Key Laboratory of Intelligent Construction and Healthy Operation and Maintenance of Deep Underground Engineering, China University of Mining and Technology. His research interests mainly focus on rock mechanics, underground engineering, and mining engineering. His contributions have been recognized with professional awards from both the government and professional associations such as the China Coal Industry Association. He has been honored with the

Youth Science and Technology Prize of the China Coal Society. He served as the session chair for international conferences/symposiums, as well as the editorial member of professional journals. Additionally, he teaches fracture mechanics at the undergraduate level, and computational solid mechanics and discontinuous mechanics at the postgraduate level.

How to cite this article: Gao Y, Cheng Y, Cai G, Gao Y, Tian J, Gao M. Corrosion effect of hydrochloric acid on the granite: insights from electrical conductivity, mineral composition, and tensile behavior. *Deep Undergr Sci Eng*. 2025;1-11. doi:10.1002/dug2.12140